NUCLEAR SCIENCE AND TECHNIQUES **26**, 060304 (2015)

Dose evaluation of therapeutic radiolabeled bleomycin complexes based on biodistribution data in wild-type rats: Effect of radionuclides in absorbed dose of different organs

Hassan Yousefnia, Samaneh Zolghadri,* Amir Reza Jalilian, and Mohammad Ghannadi-Maragheh
Nuclear Science and Technology Research Institute (NSTRI), Tehran 14395-836, Iran
(Received January 5, 2015; accepted in revised form February 5, 2015; published online December 20, 2015)

Bleomycins (BLMs), as tumor-seeking antibiotics, have been used for over 20 years in treatment of several types of cancers. Several radioisotopes are used in radiolabeling of BLMs for therapeutic and diagnostic purposes. An important points in developing new radiopharmaceuticals, especially therapeutic agents, is the absorbed dose delivered in critical organs. In this work, absorbed dose to organs after injection of ^{153}Sm-, ^{177}Lu- and ^{166}Ho-labeled BLM was investigated by radiation dose assessment resource (RADAR) method based on biodistribution data in wild-type rats. The absorbed dose effect of the radionuclides was evaluated. The maximum absorbed dose for the complexes was observed in the kidneys, liver and lungs. For all the radiolabeled BLMs, bone and red marrow received considerable absorbed dose. Due to the high energy beta particles emitted by ^{166}Ho, higher absorbed dose is observed for ^{166}Ho-BLM in the most organs. The reported data can be useful for the determination of the maximum permissible injected activity of the radiolabeled BLMs in the treatment planning programs.

Keywords: ^{166}Ho, ^{177}Lu, ^{153}Sm, Bleomycin, Dosimetry

DOI: 10.13538/j.1001-8042/nst.26.060304

I. INTRODUCTION

Nowadays, numerous chemotherapy drugs have been introduced with a different method for killing cancer cells [1]. Antitumour antibiotics are one class of chemotherapeutic agents that bind to DNA duplexes, interfering with replication and transcription of DNA, eventually leading to cell death [2].

The tumor-seeking antibiotics of bleomycins (BLMs) have been used for over 20 years for treatment of testicular cancer, lymphoma, cervical cancer and cancers of the head and neck [3, 4]. It is also used for the treatment of pleural effusions, to keep fluid from building up between the lungs and chest wall [5].

It has been indicated that BLM blocks DNA synthesis and is capable of initiating single-stranded and double-stranded cleavage of DNA through formation of an intermediate iron complex [6]. The cells are most sensitive to BLM during the G2 and M-phases of the cell cycle. There are three functional components in its molecule. The galactose and mannose derivatives may be responsible for tumour cell recognition, while the metal-chelating part could explain the anti-tumour activity of this organometallic compound. The terminal part of the molecule is probably responsible for the DNA cleavage in tumour cells [7].

Several radioisotopes have been used in radiolabeling of BLMs for therapeutic and diagnostic purposes. Bleomycin produces suitable and stable complexes with cations like Mg^{2+} Ca^{2+}, Fe^{2+}, In^{3+} etc. at the denoted sites in Fig. 1. All forms of BLM (including A_2, B_2) contains this moiety and react with metals. Comparative study indicated that ^{57}Co-BLM scintigraphy is more suitable for detecting and staging lung cancer than ^{67}Ga-citrate [8]. [^{111}In]-BLM complex also showed high *in vitro* and *in vivo* stability and demonstrated tumors more distinctly compared to ^{67}Ga-citrate [9].

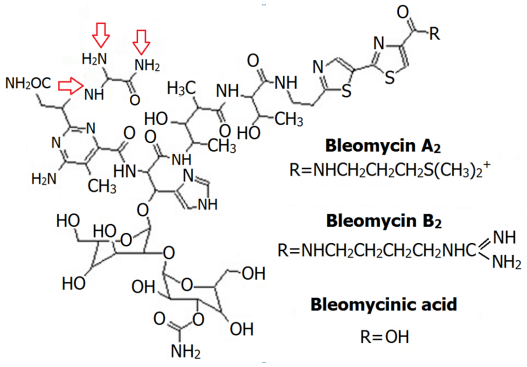

Fig. 1. (Color online) Chemical structure of BLM and its binding moiety to metals.

Complexes of BLM with β emitter radionuclides of ^{153}Sm, ^{177}Lu and ^{166}Ho have been reported recently [10–12]. While significant accumulation in human breast cancer murine xenografts was demonstrated with ^{153}Sm-BLM [13], the absorbed dose of BLM complexes in each organ has not been reported so far. In this work, due to the direct relationship between absorbed dose and the effect of radiopharmaceuticals in the management of disease, the absorbed dose to each human organ after injection of ^{153}Sm, ^{177}Lu and ^{166}Ho labeled BLM was investigated by radiation dose assessment resource (RADAR) method based on biodistribution data in wild-type rats.

II. EXPERIMENTAL SECTION

Radioisotopes were produced by irradiating targets of enriched $^{152}Sm_2O_3$ and $^{176}Lu_2O_3$, and natural $^{165}Ho(NO_3)_3$, at

* Corresponding author, szolghadri@aeoi.org.ir

a thermal neutron flux of approximately 4×10^{13} n/(cm^2 s). Whatman No. 3 paper (Whatman, UK) was used. Radiochromatography was performed by using a Bioscan AR-2000 radio TLC scanner instrument (Bioscan, France). Analytical HPLC to determine the radiochemical purity was performed by a Shimadzu LC-10AT, equipped with two detector systems, flow scintillation analyzer (Packard-150 TR) and UV-visible (Shimadzu) using Whatman Partisphere C-18 column 250 mm × 4.6 mm (Whatman Co., NJ, USA). A high purity germanium (HPGe) detector coupled with a Canberra^{TM} (model GC1020-7500SL, Canberra Industries, Inc. CT, U.S.A.) multichannel analyzer and a dose calibrator ISOMED 1010 (Elimpex-Medizintechnik, Austria) was used for counting distributed activity in rat organs. All other chemical reagents were purchased from Merck (Germany). All values were expressed as mean ± standard deviation and the data were compared using Student's T-test. Animal studies were carried out in accordance with the United Kingdom Biological Council's Guidelines on the Use of Living Animals in Scientific Investigations, 2nd ed. The wild-type rats, all weighing 180–200 g were acclimatized at proper rodent diet.

A. Production and quality of $^{153}SmCl_3$, $^{177}LuCl_3$ and $^{166}LuCl_3$ solutions

^{153}Sm, ^{177}Lu and ^{166}Ho were produced by neutron irradiation of 100 µg of the $^{152}Sm_2O_3$, Lu_2O_3 and $^{165}Ho_2O_3$ targets according to reported procedure [14] at a thermal neutron flux of 4×10^{13} n/(cm^2 s) for 5 days. The irradiated targets were dissolved in 200 µL of 1.0 mol/L HCl and diluted to the appropriate volume with ultra-pure water, to produce a stock solution. The mixture was filtered through a 0.22 µm biological filter and sent for use in the radiolabeling step. Radionuclidic purity of the solution was checked using beta and HPGe spectroscopy to detect various interfering beta- and gamma-emitting radionuclides. The radiochemical purity was checked by instant thin layer chromatography (ITLC) method.

B. Preparation of radio-labeled BLM

Radiolabeling of BLM using cation solution was performed according to the previously reported literature [10]. A stock solution was prepared by dissolving 1 mg of BLM in 1 ml normal saline. 100 µL of the stock solution was added to 100–200 MBq of the radionuclide solution. The mixture was maintained for 120 min at room temperature and the radiochemical purity was checked by ITLC method on Whatman No. 3 paper with 10 mmol/L DTPA solution as mobile phase every 15 min. HPLC of the final preparation was also performed on the reverse stationary phase using a mixture of water:acetonitrile 1 : 1 (V/V) as the eluent (flow rate: 1 mL/min). The final solution was then passed through a 0.22 µm filter and pH was adjusted to 5.5 by the addition of 1 mol/L sodium acetate buffer.

1. *Stability studies*

Stability of the radiolabeled complexes at room temperature and in human serum were checked according to the conventional ITLC method. Approximately 37 MBq of the complexes were kept at room temperature for 48 h while being checked by ITLC at specified time intervals. For serum stability studies, 37–37 MBq of the radiolabeled complexes were added to 500 mL of freshly prepared human serum and the mixture was incubated at 37 °C for 48 h, aliquots were analyzed by ITLC method.

2. *Biodistribution studies in wild-type rats*

The final transparent solutions of 50–100 µL, with 3.7 MBq radioactivity, were injected intravenously to the rats through their tail vein. The animals were sacrificed at the exact time intervals (five rats for each interval time). The activity concentration (A) of each tissue was calculated using an HPGe detector as [15],

$$A = \frac{N}{\varepsilon\gamma t_s m k_1 k_2 k_3 k_4 k_5}, \tag{1}$$

where, ε is the efficiency at photopeak energy, γ is the emission probability of the gamma line corresponding to the peak energy, t_s is the live time of the sample spectrum collection in seconds, m is the mass (kg) of the measured sample, k_1 is decay correction factor from the sample collection to the start of measurement, k_2 is decay correction factor during counting period, k_3 is self-attenuation factor in the measured sample, k_4 is pulses loss factor due to random summing, and k_5 is the coincidence factor, and N is the corrected net peak area of the corresponding photopeak given as,

$$N = N_s \frac{t_s}{t_b} N_b, \tag{2}$$

where N_s is the net peak area in the sample spectrum, N_b is the corresponding net peak area in the background spectrum and t_b is the live time of the background spectrum collection in seconds.

The percentage of injected dose per gram (%ID/g) for different organs was calculated by dividing of the activity concentration of each tissue (A) to the injected activity and the mass of each organ. All values were expressed as mean ± standard deviation and the data were compared using Student's T-test.

3. *Dosimetric studies*

The absorbed dose of each human organ was calculated by RADAR method based on biodistribution data in wild-type rats. The accumulated activity in animals was extrapolated to the accumulated activity in humans by the proposed method

of Sparks *et al*. [16], as shown in Eq. (3):

$$\widetilde{A}_{\text{human organ}} = \widetilde{A}_{\text{animal organ}} \frac{OrganMass_{\text{human}}/BodyMass_{\text{human}}}{OrganMass_{\text{animal}}/BodyMass_{\text{animal}}}, \quad (3)$$

where $\widetilde{A}$ is the accumulated activity in the source organs.

The accumulated source activity for each organ of animals was calculated by plotting the percentage-injected dose versus time for each organ and computing the area under the curves. For this purpose the data points which represent the percentage-injected dose were created. Linear approximation between the two experimental points of times was used. The curves were extrapolated to infinity by fitting the tail of each curve to a monoexponential curve with the exponential coefficient equal to physical decay constant of radioisotopes. In order to extrapolate this accumulated activity to human, the mean weights of each organ for standard human were used [17].

The absorbed dose (D in mGy/MBq) was calculated by RADAR formulation,

$$D = N \cdot DF, \quad (4)$$

where N is the number of disintegrations that occur in a source organ (in Bq s/Bq), and DF (in mGy/(MBq s)) is defined as:

$$DF = \frac{k \sum_i n_i E_i \phi_i}{m}, \quad (5)$$

where, n_i is the number of radiations emitted per nuclear transition, E_i is the energy per radiation (MeV), ϕ_i is the fraction of energy emitted that is absorbed in the target, m is the mass of target region (kg) and k is proportionality constant (mGy kg/(MBq s MeV)). In this study DFs was taken from the OLINDA/EXM software [18].

III. RESULTS AND DISCUSSION

A. Radionuclide production

Radionuclidic purity of the solutions was checked by counting the samples on an HPGe detector for 5 h. All of the radionuclides were prepared with the radionuclidic purity of over 99.98%. The radiochemical purity was checked by the two solvent systems. In 10 mmol/L DTPA aqueous solution (Solvent 1), free cation was complexed to more lipophilic LuDTPA form and migrated to higher R_f. On the other hand, in 10% ammonium acetate : methanol mixture (1 : 1) (Solvent 2), free cation remains at the origin, while other ionic species would migrate to higher R_f.

B. Preparation of radio-labeled BLM

In order to achieve maximum complexation yield, various parameters such as the ligand concentration, pH of the reaction mixture and incubation time were optimized. A satisfactory labeling yield of 94%–97% was obtained at room temperature using 0.15–0.3 mg of BLM. The best pH for the labeling step was 5.5–7.

The ratio of the peaks of the radiolabeled-BLM complexes at $R_f = 0.1$ to free cation radiopeak ($R_f = 0.8$) was considered as the radiochemical yield using 10 mmol/L DTPA solution (Fig. 2). HPLC analysis showed that the fast eluting compound was hydrophilic free cation (2.9 min), while the radiolabeled-BLM was eluted after 15.51 min (Fig. 3).

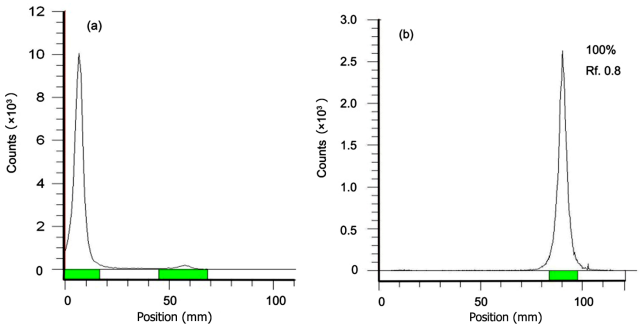

Fig. 2. (Color online) Radio chromatogram of free cation (a) and radiolabeled-BLM (b) in 10 mmol/L DTPA solution (pH 3) in optimum conditions.

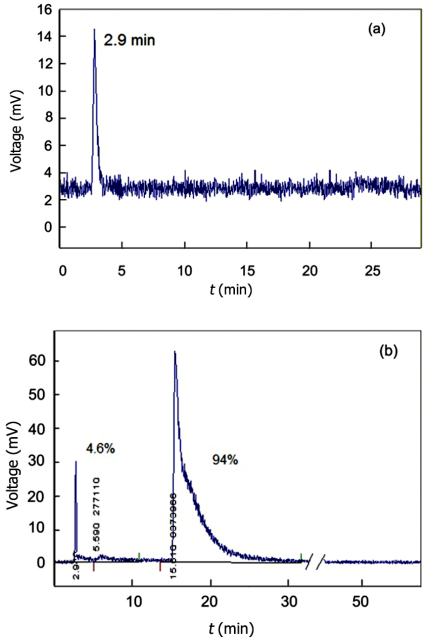

Fig. 3. (Color online) HPLC chromatogram for free cation (a), and radiolabeled-BLM (b).

C. Stability studies

Stability of the complexes prepared under optimized reaction conditions were studied at room temperature and in presence of human serum at 37 °C. It was observed that the

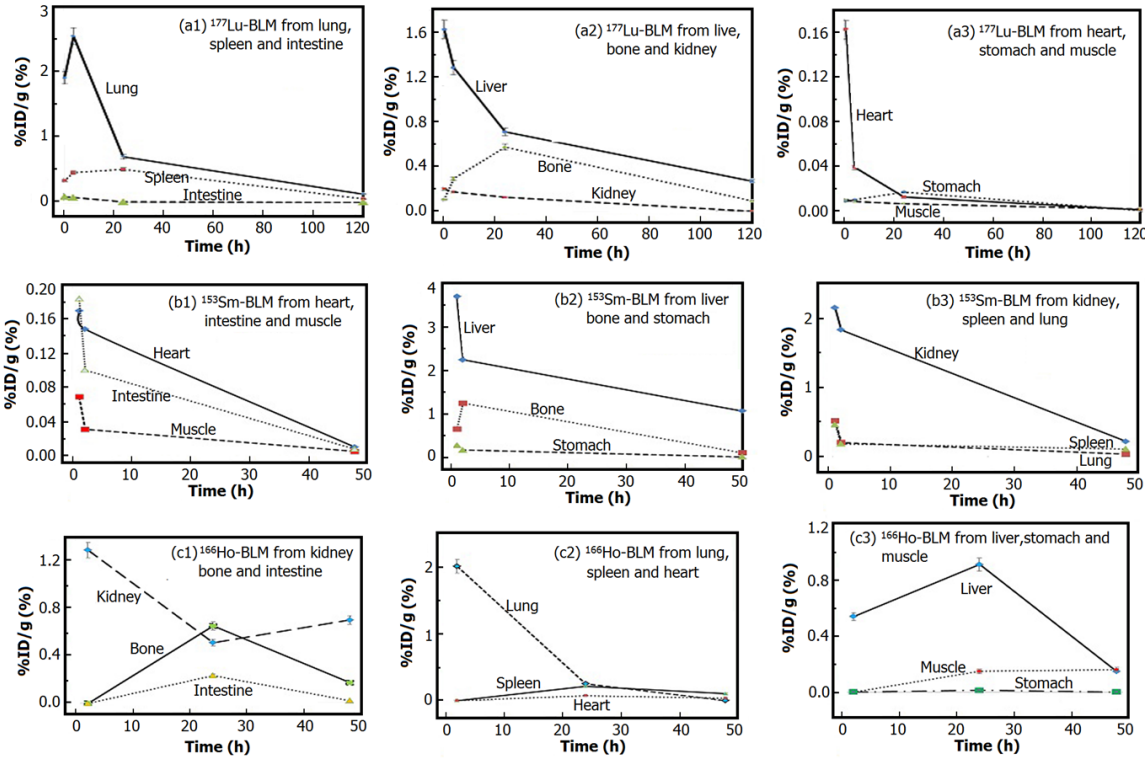

Fig. 4. (Color online) The clearance curves for ^{177}Lu-BLM (a), ^{153}Sm-BLM (b) and ^{166}Ho-BLM from each organ of the rats.

complexes showed excellent stability both at room temperature and in presence of human serum at 37 °C even after 48 h.

D. Biodistribution studies in wild-type rats

The animals were sacrificed by CO_2 asphyxiation at selected hours after injection. Dissection began by drawing blood from the aorta, followed by collecting heart, spleen, muscle, brain, bone, kidneys, liver, intestine, stomach, lung and skin samples. Tissue uptakes of the complexes were calculated as the percentage of area under the curve of the related photo peak per gram of tissue (% ID/g). The non-decay corrected clearance curves for the main organ sources of the rats are shown in Fig. 4.

The liver and kidney were the major accumulation sites of the radiolabeled BLMs. Most of the injected dose was excreted from kidneys, which is similar to the free BLM biokinetic [19]. Significant accumulation was observed in the lung, too, due to the reported side effects for this antibiotic [20, 21]. Slight bone uptake can be attributed to the small amounts of free cation in the injected sample or complex dissociation.

For comparing behaviors of the radiolabeled BLMs, tissue uptakes in the bone, kidney, liver and lung in 2–48 h after injection were studied. As demonstrated in Fig. 5, biokinetics of the radiolabeled BLMs in bone and lung follow a similar pattern. However, accumulation of ^{153}Sm-BLM in lung is significantly low and can be disregarded. The biokinetic pattern of the radiolabeled BLMs in kidney differ from that of the radiolabeled BLMs in liver. For ^{166}Ho-BLM, the renal excretion reaches its maximum at 48 h, accumulation of ^{153}Sm-BLM and ^{177}Lu-BLM in kidney decreases with time. Liver uptake for ^{153}Sm-BLM is considerably higher than the other complexes (Fig. 5).

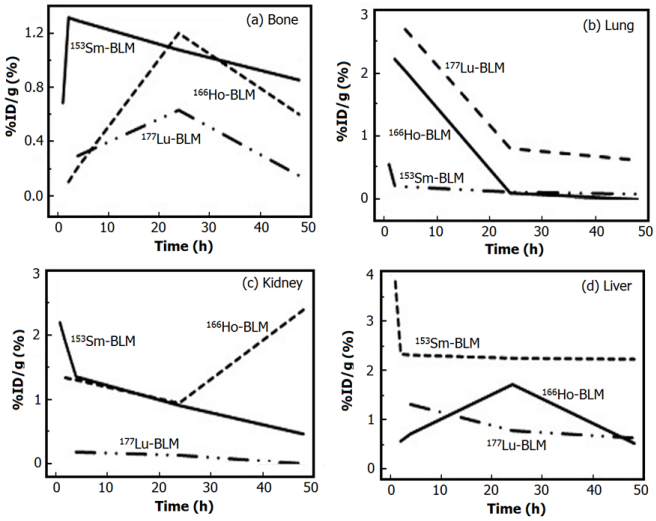

Fig. 5. Activities of ^{166}Ho-BLM, ^{153}Sm-BLM and ^{177}Lu-BLM in bone, lung, kidney and liver of wild-type rats.

Since BLMs are tumour-seeking antibiotics, biodistribution studies of the radiolabeled BLMs are suggested in tumour bearing rodents. In this study, due to the inaccessibility

to the large number of tumour bearing rats, biodistribution of the radiolabeled BLMs are studied in normal rodents.

E. Dosimetric studies

Biological study is necessary to investigate effect of radiopharmaceutical in treatment of the disease, but due to the direct relationship between absorbed dose and response in terms of cell killing/survival, calculation of the radiation absorbed dose is an important parameter to be considered [22]. Therefore, absorbed dose of the radiolabeled BLMs for each human organ was calculated by RADAR method based on biodistribution data in rat organs (Table 1). Calculation of the absorbed dose in human organs from biodistribution in small animals can be useful for determining the injected activity and is a common first step, consistent with the recommendations of ICRP 62 [23].

TABLE 1. Absorbed dose (in mGy/MBq) in each human organ after injection of the radiolabeled BLMs

Organ	^{177}Lu-BLM	^{153}Sm-BLM	^{166}Ho-BLM
Lower large intestine	0.009 ± 0.001	0.009 ± 0.000	0.011 ± 0.001
Stomach	0.002 ± 0.000	0.011 ± 0.001	0.048 ± 0.003
Heart	0.003 ± 0.000	0.010 ± 0.001	0.038 ± 0.001
Kidneys	0.019 ± 0.001	0.170 ± 0.005	0.361 ± 0.008
Liver	0.124 ± 0.007	0.560 ± 0.010	0.051 ± 0.004
Lungs	0.100 ± 0.003	0.072 ± 0.002	0.393 ± 0.009
Muscle	0.004 ± 0.000	0.008 ± 0.000	0.012 ± 0.001
Red Marrow	0.143 ± 0.005	0.208 ± 0.010	0.362 ± 0.011
Cortical Bone	0.340 ± 0.009	0.509 ± 0.012	0.449 ± 0.007
Trabecular Bone	0.434 ± 0.007	0.599 ± 0.010	0.513 ± 0.008
Spleen	0.075 ± 0.002	0.053 ± 0.001	0.123 ± 0.004
Total Body	0.033 ± 0.001	0.060 ± 0.001	0.145 ± 0.005

As indicated in Table 1, most of the organs receive the minimum absorbed dose after injection of ^{177}Lu-BLM, while the maximum absorbed dose was observed after injection of ^{166}Ho-BLM. In addition to the different biodistribution of the radiolabeled BLMs, the difference in absorbed dose is attributed to the decay characteristics of the radionuclides. ^{166}Ho ($E_{\beta\,\max} = 1.84$ MeV, $T_{1/2} = 26.8$ h), ^{153}Sm ($E_{\beta\,\max} = 0.81$ MeV, $T_{1/2} = 46.3$ h) and ^{177}Lu ($E_{\beta\,\max} = 0.497$ MeV, $T_{1/2} = 161.52$ h) are interesting radionuclides for targeted therapy modalities for treatment of the large, medium and small sized tumors, respectively. Therefore, the higher amount of the absorbed dose of ^{166}Ho-BLM can be considered as a result of the high energy beta particles.

Generally, the organs with the maximum absorbed dose after injection of the radiolabeled BLMs are the kidney, liver, lung, red marrow and bones. In the case of ^{166}Ho-BLM, the kidneys and lungs are the critical organs which can restrict the injected activity. However, for ^{177}Lu-BLM and ^{153}Sm-BLM, liver receive higher absorbed dose than lungs and it can be considered as a critical organ. Furthermore, for all the radiolabeled BLMs, due to the slight bone uptake, significant absorbed dose was observed in red marrow. However, with respect to the high energy beta particles emitted from ^{166}Ho, red marrow absorbed dose is considerably higher (0.362 versus 0.208 and 0.143 mSv/MBq for ^{153}Sm-BLM and ^{177}Lu-BLM, respectively). These calculated radiation absorbed dose can be used for the treatment planning of radiotherapy with the radiolabeled BLMs as a preliminary dose data.

IV. CONCLUSION

According to the results, radiolabeled BLMs were prepared with high radiochemical purity and can be good candidates for the treatment of various malignancies. Significant accumulation was obtained in lungs which can be considered as a side-effect of these complexes. Due to the high energy of the emitted beta particles of ^{166}Ho, higher absorbed dose is observed for ^{166}Ho-BLM in the most organs. However, absorbed dose of ^{166}Ho-BLM in the liver is considerably lower than the other complexes, but the red marrow and lungs received considerably higher absorbed dose. Generally, lungs, liver, kidneys and red marrow are the major dose-limiting tissues. According to the threshold amount of absorbed dose for critical organs, the obtained results can be useful for the determination of the maximum permissible injected activity of the radiolabeled BLMs in the treatment planning programs.

[1] Payne S and Miles D. Mechanisms of anticancer drugs. In: Gleeson M and Clarke R C. Scott–Brown's Otorhinolaryngology: Head and neck surgery, 2008, 34–46.

[2] Drugs: How Chemotherapy Works. https://acco.org/Information/drugsaction.aspx/

[3] Fu K K, Phillips T L, Silverberg I J, *et al*. Combined radiotherapy and chemotherapy with bleomycin and methotrexate for advanced inoperable head and neck cancer: update of a Northern California Oncology Group randomized trial. J Clin Oncol, 1987, **5**: 1410–1418.

[4] Bokemeyer C. Bleomycin in testicular cancer: Will pharmacogenomics improve treatment regimens? J Clin Oncol, 2008, **26**: 1783–1785. DOI: 10.1200/JCO.2007.15.2991

[5] Antunes G, Neville E, Duffy J, *et al*. BTS guidelines for the management of malignant pleural effusions. Thorax, 2003, **58**: 29–38. DOI: 10.1136/thx.58.suppl_2.ii29

[6] Harsch A, Marzilli L A, Bunt R C, *et al*. Accurate and rapid modeling of iron-bleomycin-induced DNA damage using tethered duplex oligonucleotides and electrospray ionization ion trap mass spectrometric analysis. Nucl Acids Res, 2000, **28**: 1978–1985. DOI: 10.1093/nar/28.9.1978

[7] Ryynänen P. Kinetic mathematical models for the ^{111}In-labelled BLM complex and ^{10}B in boron neutron capture therapy. Report series in physics Helsinki, 2002.

[8] Nieweg O E, Beekhuis H, Piers D A, *et al*. ^{57}Co-bleomycin and ^{67}Ga-citrate in detecting and staging lung cancer. Thorax,

1983, **38**: 16–21. DOI: 10.1136/thx.38.1.16
[9] Hou D, Hoch H, Johnston Gs, *et al*. A new tumor imaging agent–^{111}In-bleomycin complex. Comparison with ^{67}Ga-citrate and ^{57}Co-bleomycin in tumor-bearing animals. J Surg Oncol, 1984, **27**: 189–195. DOI: 10.1002/jso.2930270313
[10] Yousefnia H, Jalilian A R, Zolghadri S, *et al*. Preparation and quality control of lutetium-177 bleomycin as a possible therapeutic agent. Nukleonika, 2010, **55**: 285–291.
[11] Zolghadri S, Jalilian A R, Yousefnia H, *et al*. Development of ^{166}Ho bleomycin as a possible therapeutic complex. J Radioanal Nucl Chem, 2010, **285**: 461–467. DOI: 10.1007/s10967-010-0589-2
[12] Bahrami-Samani A, Ghannadi-Maragheh M, Jalilian A R, *et al*. Development of 153Sm-bleomycin as a possible therapeutic complex. Nucl Sci Tech, 2010, **21**: 165–1709. DOI: 10.13538/j.1001-8042/nst.21.165-170
[13] Bahrami-Samani A, Ghannadi-Maragheh M, Jalilian A R, *et al*. Biological studies of samarium-153 bleomycin complex in human breast cancer murine xenografts for therapeutic applications. Radiochim Acta, 2010, **98**: 237–242. DOI: 10.1524/ract.2010.1713
[14] International Atomic Energy Agency. Manual for reactor produced radioisotopes. Vienna, Austria, IAEA-TECDOC-1340, 2003.
[15] International Atomic Energy Agency. Quantifying uncertainty in nuclear analytical measurements. Vienna, Austria, IAEA-TECDOC-1401, 2004.
[16] Sparks R B and Aydogan B. Comparison of the effectiveness of some common animal data scaling techniques in estimating human radiation dose. Sixth International Radiopharmaceutical Dosimetry Symposium, Oak Ridge, TN: Oak Ridge Associated Universities, 1996, 705–716.
[17] Stabin M G and Siegel J A. Physical models and dose factors for use in internal dose assessment. Health Phys, 2003, **85**: 294–310.
[18] Stabin M G, Sparks R B and Crowe E. OLINDA/EXM: The second-generation personal computer software for internal dose assessment in nuclear medicine. J Nucl Med, 2005, **46**: 1023–1027.
[19] Thakur M L. The preparation of Indium-111 labelled bleomycin for tumour localization. Int J Appl Rad Isot, 1973, **24**: 357–359.
[20] Meadors M, Floyd J and Perry M C. Pulmonary toxicity of chemotherapy. Semin Oncol, 2006, **33**: 98–105. DOI: 10.1053/j.seminoncol.2005.11.005
[21] O'Sullivan J M, Huddart R A, Norman A R, *et al*. Predicting the risk of bleomycin lung toxicity in patients with germ-cell tumours. Ann Oncol, 2003, **14**: 91–96. DOI: 10.1093/annonc/mdg020
[22] Talwer G P and Srivastava L M. Textbook of biochemistry and human biology. New Delhi (India): Prentice-Hall of India Pvt.Ltd, 2004.
[23] ICRP. ICRP Publication 62: Radiological protection in biomedical research. Annals of the ICRP, 1992, 22.